Acc. Chem. Res. **2001,** *34,* 239−247

New Materials in Hydrothermal Synthesis

SHOUHUA FENG AND RUREN XU*
Key Laboratory of Inorganic Synthesis and Preparative Chemistry, Department of Chemistry, Jilin University, Changchun 130023, P. R. China

Received April 17, 2000

ABSTRACT
In this Account we describe the hydrothermal synthesis of some new materials including microporous crystals, ionic conductors, complex oxides and fluorides, low-dimensional aluminophosphates, inorganic−organic hybrid materials, and particularly condensed materials such as diamond and inorganic helical chains. Hydrothermal synthesis in biology and environment sciences is also introduced. The increasing interest in hydrothermal synthesis derives from its advantages in terms of high reactivity of reactants, easy control of solution or interface reactions, formation of metastable and unique condensed phases, less air pollution, and low energy consumption.

Introduction

Hydrothermal synthesis refers to the synthesis by chemical reactions of substances in a sealed heated solution above ambient temperature and pressure. It involves the preparation of new materials, the understanding of mechanisms of hydrothermal reactions, and the development of novel synthetic methods and techniques. Understanding the mechanism of hydrothermal reactions is particularly necessary for both the suitable application of a method to a specific synthesis and the exploration of new materials with desired properties. Basically, the mechanism of hydrothermal reactions follows a liquid nucleation model.[1] It is different from that of solid-state reactions, where the reaction mechanism involves mainly diffusion of atoms or ions at the interface between reactants. However, in the supercritical region of water, less data are available at present, and only those for pure water and simple saltwater solutions are known. New methods and strategies play an important role in the investigation of hydrothermal synthesis. The various methods such as induced growth through crystal seeds, structure-directing agent technique, mineralizing, templating, complexing, nonaqueous solvothermal routes, high temperature and pressure technique, and redox environment control make hydrothermal reactions particularly available for new advanced solid materials.[2]

Hydrothermal synthesis has been successful for the preparation of important solids such as microporous crystals,[3] superionic conductors,[4] chemical sensors,[5] electronically conducting solids,[6] complex oxide ceramics and fluorides,[7,8] magnetic materials,[9] and luminescence phosphors.[10] It is also a route to unique condensed materials including nanometer particles, gels, thin films, equilibrium defect solids, distinguished helical and chiral structures, and particularly-stacking-sequence materials. In addition to the synthesis of new materials, hydrothermal synthesis has been important in biology and environmental sciences, for examples, in the origin of life[11,12] and in the supercritical water oxidation process for decomposing organic wastes.[13]

In this Account we describe the hydrothermal synthesis of some new materials including microporous crystals, ionic conductors, complex oxides and fluorides, low-dimensional aluminophosphates, inorganic−organic hybrid materials, and unique condensed materials such as diamond and inorganic helices. Hydrothermal synthesis in biology and environment sciences is also introduced.

Microporous Crystals

Zeolites are basically prepared from hydrothermal systems. Traditionally, they refer to a class of microporous crystalline aluminosilicates with TO_4 (T = Si or Al) tetrahedra as basic building units. The discovery of high-silica zeolites, sometimes the so-called pure SiO_2 zeolites, namely silicalites I and II, by the use of organic molecules in synthesis introduced the new concept of a "templating agent". These compounds are mainly amines and organic ammonium ions such as tetrapropylammonium ions in the synthesis of ZSM-5.[3] Microporous aluminophosphates ($AlPO_4$-n) developed by Wilson et al.[14] at Union Carbide are a new family of neutral framework zeolites. However, most of the framework structures such as types A, Y, and ZSM-5 developed before $AlPO_4$-n were constructed from TO_4 tetrahedra (T = Si, Al, and P). The application of these zeolites to catalysis was based on the utilization of their large intersurface areas, channel shape-selectivities, and acidic properties.

The variety of the microporous crystals was extremely enlarged due to the appearance of mixed TO_3, TO_4, TO_5, and TO_6 basic building blocks involved in the frameworks. Starting with a structural observation of some microporous gallophosphates, in which mixed four-, five-, and six-coordinate Ga atoms were found by Parise,[15] a number of new microporous crystals were prepared from $R-Ga_2O_3-P_2O_5-H_2O$ and $R-M(I,II)-Al_2O_3-B_2O_3-H_2O$ systems (where R is a template such as an organic amine and M is a monovalent alkali or divalent alkaline earth

Shouhua Feng, born in 1956 in Jilin, B.S., M.S., and Ph.D. from Jilin University, worked at Rutgers University and Aberdeen University. Since 1992 he has been Professor in the Chemistry Department, Jilin University. His research interests include hydrothermal and solvothermal syntheses of microporous crystals, inorganic functional solids, and inorganic−organic hybrid materials. He received an award from the National Outstanding Youth Fund of China in 1994. He is currently a Director of the Key Laboratory of Inorganic Synthesis and Preparative Chemistry and holds a Specially-Appointed Professorship from the Education Ministry of China.

Ruren Xu, born in 1932 in Zhejiang, B.S. from National Shanghai Jiaotong University, worked at Fu Dan University and Hamburg University. Since 1979, he has been Professor in the Department of Chemistry, Jilin University. His research interests includes hydrothermal and solvothermal syntheses of microporous crystals, low-dimensional aluminophosphates, bioinorganic materials, and combinatorial molecular engineering. He is currently an Academician of the Chinese Academy of Sciences, Councilor of the International Zeolite Association, and Committee Member of the National Nature Science Foundation of China (NSFC).

10.1021/ar0000105 CCC: $20.00
Published on Web 12/20/2000

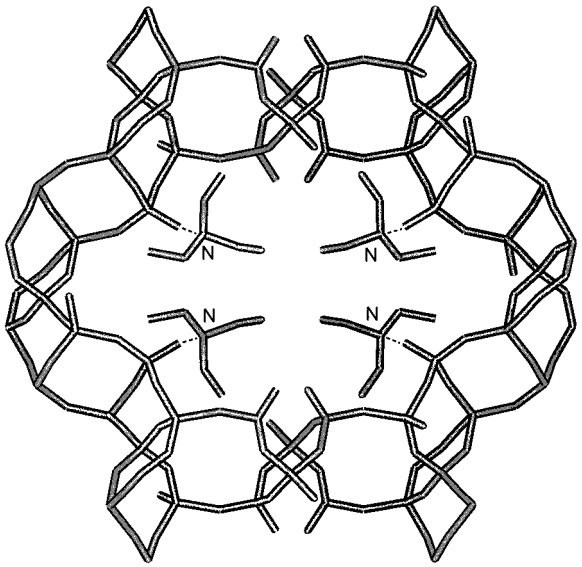

FIGURE 1. Structure of JDF-20 (template molecules interact with terminal oxygen atoms through H-bonds as indicated by the fine lines). Reprinted with permission from ref 46. Copyright 2000 Elsevier.

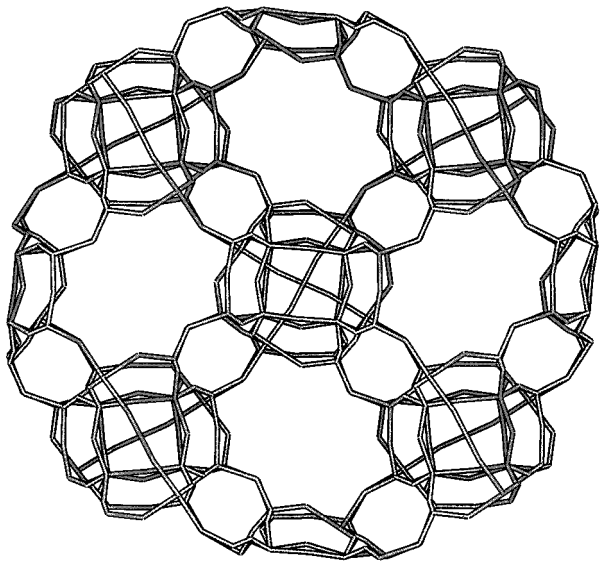

FIGURE 2. Open framework of AlPO−CJB1 along the [001] direction. Reprinted in part with permission from ref 26. Copyright 2000 American Chemical Society.

metal) by our group, including $GaPO_4-C_n$, $n = 1-12$,[16,17] and microporous aluminoborates, $B-C_n$, $n = 1-10$.[18] Moreover, the 18-membered ring VPI-5,[19] 20-membered ring microporous Cloverite,[20] and 24-membered ring zinc phosphate ND-1[21] were also reported. A new microporous titanosilicate, JLU-1, was recently synthesized in a $SiO_2-TiO_2-Na_2O-H_2O-(TMA)_2O$ system;[22] its framework is composed of tetrahedral SiO_4 and octahedral TiO_6. High-resolution transmission electron microscopy revealed its microporosity for a uniform window size of ca. 6.0 Å.

Following the first discovery of silica sodalite from nonaqueous systems by Bibby and Dale,[23] a large number of new compositions were prepared, including zeolites containing five-membered-rings[24] and a 20-membered ring microporous crystal, JDF-20, $[Al_5P_6O_{24}H]\cdot 2[Et_3NH]\cdot 2H_2O$.[25] JDF-20 was prepared with triethylene glycol (TEG) as the solvent of the reaction system and Et_3N as the template; it has a three-dimensional (3D) framework with Al/P ratio of 5/6 and consists of 20-membered ring channels with an elliptical aperture (6.2 Å × 7.9 Å), as shown in Figure 1. An unusual microporous aluminophosphate with an anionic framework, $[Al_{12}P_{13}O_{52}]^{3-}[(CH_2)_6N_4H_3]^{3+}$, denoted AlPO−CJB1, possesses Brönsted acidity upon removal of its template molecules at 600 °C.[26] AlPO−CJB1 was prepared from nonaqueous systems containing ethylene glycol solvent and hexamethylenetetraamine template. Its open framework along the [001] direction is shown in Figure 2. The Brönsted acidity originates from the existence of AlO_5 units and protons from the decomposition of the template.

Ionic Conductors

Co-doped nanocrystalline ceria-based compositions, $Ce_{1-x}M_xBi_{0.4}O_{2.6-x}$, M = Ca, Sr, and Ba, $x = 0.01-0.15$, serve as good examples for describing the hydrothermal synthesis and doping for ionic conductors.[27,28] CeO_2-based materials doped with aliovalent cations show promising ionic transport properties in application to solid oxide fuel cells and oxygen pumps. Pure phase $CeO_{2-\delta}$ with the cubic fluorite structure shows mixed electronic and ionic conduction, and the introduction of lower-valence metal ions into the lattice of CeO_2 greatly improves their ionic conduction due to the quantitative formation of oxygen vacancies and in some cases eliminates its electronic conduction.

The synthesis and doping strategy was based on the hydrothermal technique. A typical synthetic procedure for $Ce_{0.9}Ba_{0.1}Bi_{0.4}O_{2.5}$ began with mixing cerium(III) nitrate hexahydrate, bismuth(III) nitrate pentahydrate, and $Ba(NO_3)_2$ with deionized water to form a solution, to which NaOH as a mineralizer was added dropwise with stirring to form a dark yellowish mixture. The mole composition of the final reaction mixture was 1.00 CeO_2:0.42 Bi_2O_3:0.05 BaO:580 H_2O:2.60 Na_2O. The mixture was sealed in Teflon-lined stainless steel autoclaves and crystallized at 240 °C for 24 h. The particle sizes of all the products were in the nanometer range due to the use of a hydrothermal synthesis technique. The ionic conductivity has been greatly enhanced in these codoped systems. The highest ionic conductivity for $Ce_{0.95}Ca_{0.05}Bi_{0.4}O_{2.55}$ at 600 °C was 1.7×10^{-2} S·cm^{-1}, which was much higher than that of the well-known Ca-stabilized zirconia and calcium monodoped ceria.

A protonic NASICON, $HZr_2P_3O_{12}$, was synthesized under hydrothermal conditions and characterized as a humidity sensor operated at relatively high temperatures.[29] Fluorite-type $Bi_{17}V_3O_{33}$ obtained from the hydrothermal system showed special superlattice structure and oxygen ion conductivity.[30] Another example is the hydrothermal synthesis of a new potassium phosphatoantimonate, $K_8Sb_8P_2O_{29}\cdot 8H_2O$, exhibiting ionic conductivity.[31]

On the other hand, with the aim to search for new microporous materials showing both channels and mobile

Table 1. List of Hydrothermally Synthesized Complex Oxides and Fluorides

materials	reaction		ref
	T (°C)	*t* (days)	
$Bi_{17}V_3O_{33}$	180	5	30
$Cu_4Bi_2V_2O_{13}$	240	3	41
$Ce_{1-x}M_xBi_{0.4}O_{2.6-x}$ (M = Ca, Sr, Ba)	240	3	27
$M_xLa_{2/3-x/3}TiO_3$ (M = Na, Li, Ag)	240	7	36
$La_{1-x}M_xMnO_3$ (M = Ca, Sr, Ba)	240	1	9
$NaMTi_2O_6$ (M = Nd, Ce)	240	3	36
$MMo(W)O_4$ (M = Ca, Sr, Ba)	240	3	36
Bi_2MO_6 (M = Mo, W)	180	5	42
$Ba_5Nb_4O_{15}$	240	1	43
$Pb_2Bi_2O_7$	140	1	38
$M_2Sn_2O_7$ (M = La, Bi, Y, Gd)	240	3	7
ABF_3 (A = Li, K; B = Ba, Mg)	140	5	8
ABF_4 (A = Li, K; B = Y, Er, Ho)	220	3	39

ion transport, we developed a number of materials exhibiting excellent ionically conducting properties, capable of ion-exchange and strong potential as chemical sensors. A series of crystalline, microporous germanates, $M_3HGe_7O_{16}{\cdot}xH_2O$ (M = NH_4^+, Li^+, Na^+, K^+, Rb^+, and Cs^+), showed considerable ionic conductivities due to their particular framework structures which are composed of $(GeO_4)_3(GeO_6)_4$ subunits where one-fourth of the oxygens were four-coordinated, contributing to a weak interaction between the mobile ions and anionic framework.[32−34] These materials have three-dimensional (3D) structures with channels where mobiled cations are located. The best ionic conductivity, 2.0×10^{-3} S·cm^{-1} at 400 °C, was found with $Cs_3HGe_7O_{16}$.[33]

Complex Oxides and Fluorides

The hydrothermal technique has been extensively applied to the syntheses of advanced inorganic materials, which are difficult or impossible to prepare by high-temperature solid-state reactions. A variety of novel hydrothermal reactions for the synthesis of advanced complex oxides and fluorides have been developed. Hydrothermal synthesis is advantageous due to the relatively mild conditions required, one-step synthetic procedure and controllable particle size distribution. Table 1 summarizes conditions for selected complex oxides and fluorides by hydrothermal synthesis in our laboratory.[35−43]

Perovskites, ABO_3 (A = Ca, Sr, Ba, Pb; B = Ti, Sn, Zr), were hydrothermally prepared;[35] complex oxides containing rare earth ions, e.g., $Na_xLa_{2/3-x/3}TiO_3$, $Na_xAg_yLa_{2/3-(x+y)/3}TiO_3$ and $Na_xLi_yLa_{2/3-(x+y)/3}TiO_3$, synthesized hydrothermally at 200−240 °C show enhanced electrical conductivity.[36] Further, giant magnetoresistance (GMR) materials, $La_{1-x}A_xMnO_3$ (A = Ca, Sr, and Ba), were recently synthesized from hydrothermal systems at 240 °C; for example, the Ba analogue, $La_{0.5}Ba_{0.5}MnO_3$, was obtained by heating an aqueous reaction mixture containing $KMnO_4$ and $MnSO_4$ reactants. $La_{0.5}Ba_{0.5}MnO_3$ began to crystallize after 2 h, and the crystallization was complete after 24 h. The valence change of Mn atoms from $KMnO_4$ and $MnSO_4$ for the formation of the product $La_{0.5}Ba_{0.5}(Mn^{3+}{}_{0.5}Mn^{4+}{}_{0.5})O_3$ is suggested to occur as follows:

$$0.5\text{Mn(VII)} + 1.5\text{Mn(II)} \rightarrow 2(Mn^{3+}{}_{0.5}Mn^{4+}{}_{0.5}) \quad (1)$$

$La_{0.5}Ba_{0.5}MnO_3$ crystallizes in cubic symmetry with a = 3.913 Å; it contains mixed-valent Mn atoms with an average valence state ca. 3.5 and exhibits giant magnetoresistance.[9]

Complex oxides with garnet[37] and pyrochlore structures,[38] such as $Sr_3M_2(OH)_{12}$, $Pb_2Bi_2O_7$, and $M_2Sn_2O_7$ (M = La, Bi, Gd, or Y), were readily synthesized from hydrothermal systems. For the $Bi_2O_3-PbO_2$ hydrothermal systems, the formation of $Pb_2Bi_2O_7$ was dependent upon the starting reagents. The use of $Bi(NO_3)_3$ and PbO_2 as the Bi and Pb sources led to a relatively simple reaction from the point of view of oxidation state changes from the reactants to products. In an alternative synthesis, $NaBiO_3$ and $Pb(NO_3)_2$ were also found to be suitable starting reagents for the formation of $Pb_2Bi_2O_7$. However, when $NaBiO_3$, PbO, and $Pb(NO_3)_2$ were employed, $Bi_2Pb_2O_7$ formed by a more complicated mechanism. In this system, the redox reactions involved in the formation of $Pb_2Bi_2O_7$ might occur as follows:

$$2NaBi^{5+}O_3 + 2Pb^{2+}O + H_2O \rightarrow Bi^{3+}{}_2Pb^{4+}{}_2O_7 + 2OH^- + 2Na^+ \quad (2)$$

$$2NaBi^{5+}O_3 + 2Pb^{2+}(NO_3)_2 + 2OH^- \rightarrow Bi^{3+}{}_2Pb^{4+}{}_2O_7 + H_2O + 2Na^+ + 4NO_3^- \quad (3)$$

$$2NaBi^{5+}O_3 + 2Pb^{4+}O_2 + H_2O \rightarrow Bi^{3+}{}_2Pb^{4+}{}_2O_7 + O_2\uparrow + 2OH^- + 2Na^+ \quad (4)$$

Complex fluorides show various interesting structures and physical properties such as piezoelectric characteristics, photoluminescence behavior, ionic conductivity, and nonmagnetic insulating behavior. The preparation of complex fluorides by high-temperature solid-state reactions was previously reported, but requirements for the synthetic apparatus due to the corrosive nature of fluorides limited the study by solid-state synthesis. Hydrothermal syntheses of $LiBaF_3$ and $KMgF_3$ with perovskite structures were carried out at 120−240 °C in the presence of a mineralizer, HF or NH_4HF_2. Crystalline $KMgF_3$ was obtained by mixing KF and MgF_2 with deionized water, adding hydrofluoric acid, and heating at 120−240 °C under autogenous pressure for several days.[8] $LiBaF_3$ was synthesized in the same way either from a reaction mixture of LiF, BaF_2, and water, or from LiOH and $Ba(OH)_2$ solutions to which NH_4HF_2 was added. As an extension, complex fluorides with scheelite and wolframite structures were hydrothermally synthesized and doped with photosensitive rare earth elements. The complex fluorides, ABF_4 (A = Li, K; B = Y, Er, Ho), were synthesized at 140−240 °C, and doping of Eu^{3+} ions in $LiYF_4$ and KYF_4 was carried out by directly adding Eu_2O_3 into the reaction mixtures.[10,39,40]

Low-Dimensional Aluminophosphates

The well-known microporous aluminophosphates, denoted $AlPO_4$-*n*, are typically built up from strict alternation

of AlO_4 and PO_4 tetrahedra to form neutral 3D frameworks with an Al/P ratio of unity. Recently, novel chains and layers of low-dimensional metal phosphates were observed in solvothermal synthesis. These low-dimensional metal phosphates, which constitute an important area of materials chemistry, are rare in nature, but in nonaqueous systems they show reasonable stability in either one-dimensional (1D) or two-dimensional (2D) forms. Among low-dimensional metal phosphates, denoted as MePOs (Me = Fe, Co, In, Zn, Ti, or Al), a number of members of a novel class of low-dimensional aluminophosphates (AlPOs) provide good examples, for they were well defined by both theoretical network modeling and experimental synthesis.[44−46] Apparently, the organic solvent plays an important role in decreasing the dimensionality in AlPOs. Part of the reason for this may be the coverage and space effects of organic solvents on certain reactive groups of aluminum and phosphor species. Indeed, in their structures various basic units of Al-centered polyhedra such as AlO_4, AlO_5, $AlO_4(OH_2)_2$, and terminal P−OH and/or P═O groups exist, leading to their Al/P ratios less than unity; the common Al/P ratios are 1/2, 3/5, 2/3, 3/4, and 4/5, and as a result, the networks are negatively charged with the empirical formula $Al_nP_{n+1}O_{4(n+1)}^{3-}$ (n = 1, 2, 3, and 4). The negative charges are compensated by protonated organic ammonium cations located in the structures. Typical stoichiometries of low-dimensional aluminophosphates are $AlP_2O_8^{3-}$, $Al_3P_5O_{20}^{6-}$, $Al_2P_3O_{12}^{3-}$, $Al_3P_4O_{16}^{3-}$, and $Al_4P_5O_{20}^{3-}$.

The $Al_3P_4O_{16}^{3-}$ layers exhibit rich structural diversity and have been found in a number of 2D compounds with different sheet structures and organic templates. There are unique six sheets constructed by 4−6−8(I), 4−6−12, 4−6(I), 4−6(II), 4−6(III), and 4−6−8(II) rings, respectively, in the following six compounds: $[Al_3P_4O_{16}]\cdot[NH_3(CH_2)_2NH_3][OH_2(CH_2)_2OH][OH(CH_2)_2OH]$, $[Al_3P_4O_{16}]\cdot3[CH_3(CH_2)_2NH_3]$, $[Al_3P_4O_{16}]\cdot1.5[NH_3(CH_2)_4NH_3]$, $[Al_3P_4O_{16}]\cdot3[CH_3(CH_2)_3NH_3]$, $[Al_6P_8O_{32}]\cdot3[NH_3CHMeCH_2NH_3]H_2O$, and $[Al_3P_4O_{16}]\cdot2[C_5N_2H_9][NH_4]$, where II and III represent different styles of combination for the same ring. The difference in their structures is the style of combination of various rings in a sheet. Figure 3 shows the six distinct 2D sheet patterns, including the combinations of 4−6−8(I), 4−6−12, 4−6(I), 4−6(II), 4−6(III), and 4−6−8(II) rings above six AlPOs. These aluminophosphate layers are held by interlammellar template cations and stack in various sequences, such as AAAA, ABAB, ABCABC, and ABCDEF. Figure 4 shows a sheet composed of the 4−6−12 rings stacked in an ABAB sequence, which creates a 12-membered ring channels along the *c*-axis in the structure of $[Al_3P_4O_{16}]\cdot1.5[NH_3(CH_2)_4NH_3]$. The numerous ring combinations and sheet stacking sequences provide the possibility to explore devised structures for catalysis and for pillared microporous materials.

Other low-dimensional $[AlP_2O_8H_2(OH_2)_2]\cdot[N_2C_3H_5]$, $[Al_2P_3O_{10}(OH)_2]\cdot[C_6NH_8]$, $[AlP_2PO_8H_2]\cdot[Et_3NH]$, and $[AlP_2O_8H]\cdot[H_3NCH_2CH_2NH_3]$ were also prepared from nonaqueous systems. These 1D chains and 2D sheets are stabilized by protonated organic amines (templates) by H-bonding interaction with certain regularity. The templating ability of various organic amines for the inorganic layers depends on the energies of the template−layer interactions. Therefore, this study provides a rational way to synthesize theoretically designed AlPOs.

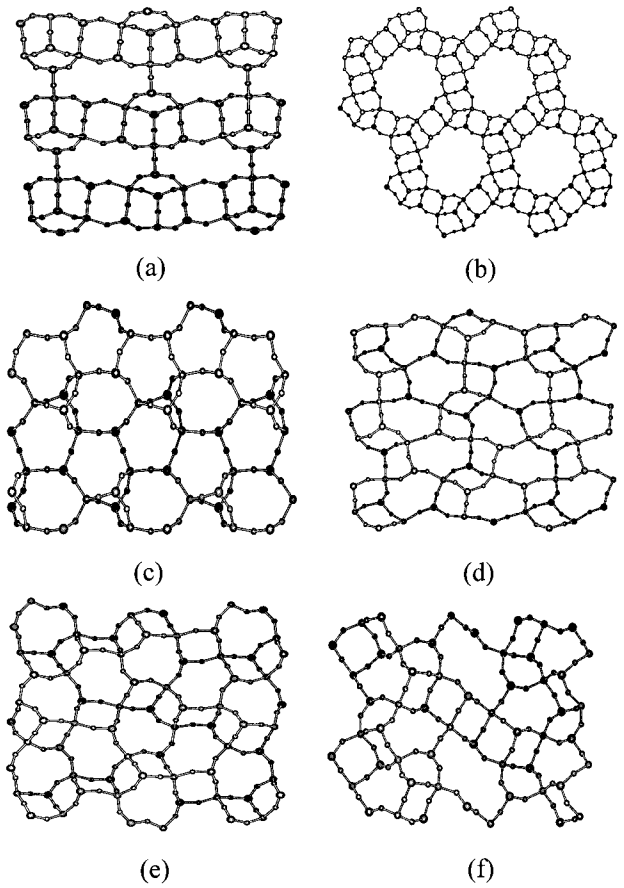

FIGURE 3. Six distinct styles of combination of (a) 4−6−8(I) rings, (b) 4−6−12 rings, (c) 4−6(I) rings, (d) 4−6(II) rings, (e) 4−6(III) rings, and (f) 4−6−8(II) rings in 2D AlPOs (terminal oxygen atoms are omitted). Reprinted with permission from ref 46. Copyright 2000 Elsevier.

Inorganic−Organic Hybrid Materials

Hydrothermal reactions have been extensively applied to the synthesis of inorganic−organic hybrid materials, such as coordination polymers and clusters. The coordination polymers and clusters, which bridge the molecular and atomic solids, possess potential functions such as enantiomer separation, chiral synthesis, ligand exchange, and selective catalysis. The coverage of this section is limited to some examples of our recent hydrothermal syntheses, for many works in the field have been well reviewed.[47−50]

Our recent efforts in this field are focused mostly on the design and hydrothermal synthesis of novel coordination polymers and clusters by using neutral donor ligands (i.e., 4,4′-bipyridine, pyrimidine, pyrazine), strictly anionic ligands (i.e., carboxylate), and their combination. For example, the hydrothermal reactions of V_2O_5, $H_2C_2O_4$, $Ni(NO_3)_2$, ethylenediamine (en) or 1,2-diaminopropane (enMe), and water yield two layered vanadium oxides with

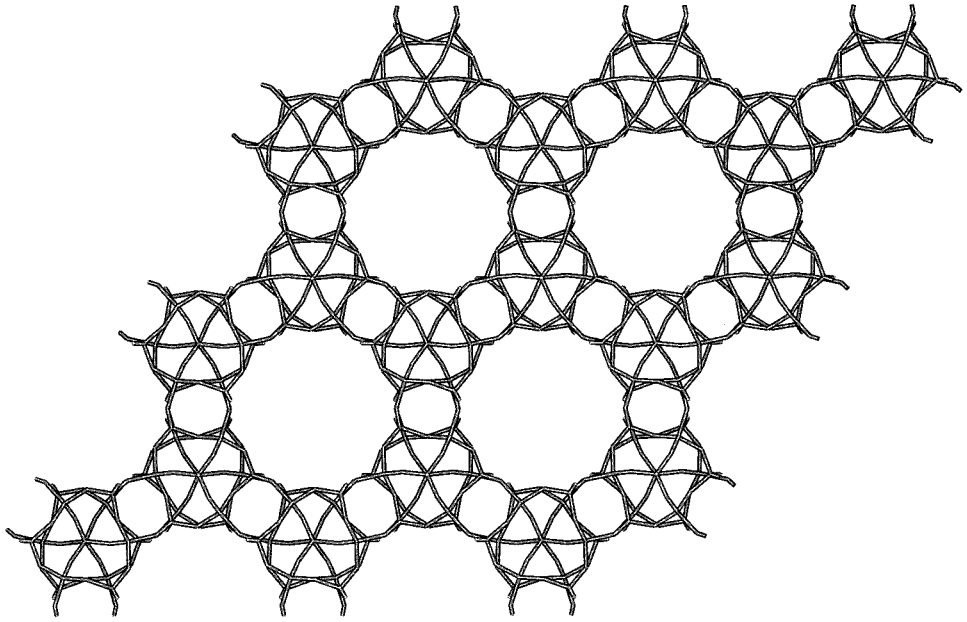

FIGURE 4. The 4−6−12 ring sheets stacked in an ABAB sequence, creating 12-membered ring channels along the *c*-axis in the structure of $[Al_3P_4O_{16}]$•$1.5[NH_3(CH_2)_4NH_3]$. Adapted from our previously published data (Thomas, J. M.; Jones, R. H.; Xu, R; Chen, J.; Chippindale, A. M.; Natarajan, S.; Cheetham, A. K. Novel Porous Sheet Aluminophosphate: $Al_3P_4O_{16}^{3-}$ $1.5[NH_3(CH_2)_4NH_3]^{2+}$. *J. Chem. Soc., Chem. Commun.* **1992**, 929−931).

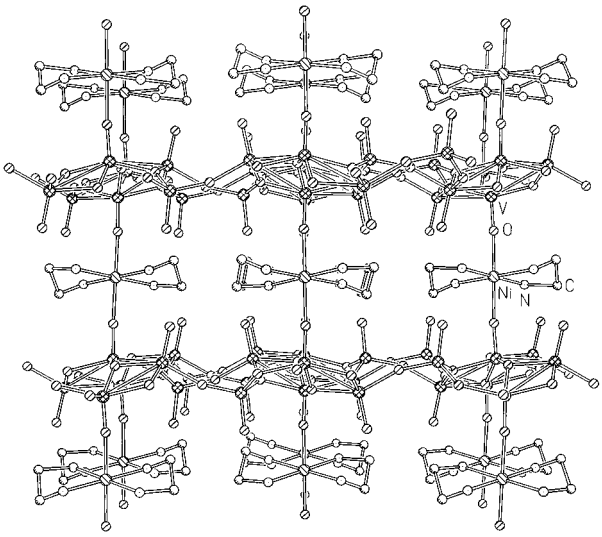

FIGURE 5. View of the structure of $[Ni(en)_2]_{0.5}[V_3O_7]$ down the *b*-axis, showing the layers of vanadium oxide with interlayer $\{Ni(en)_2\}^{2+}$. Reprinted with permission from ref 51. Copyright 1999 American Chemical Society.

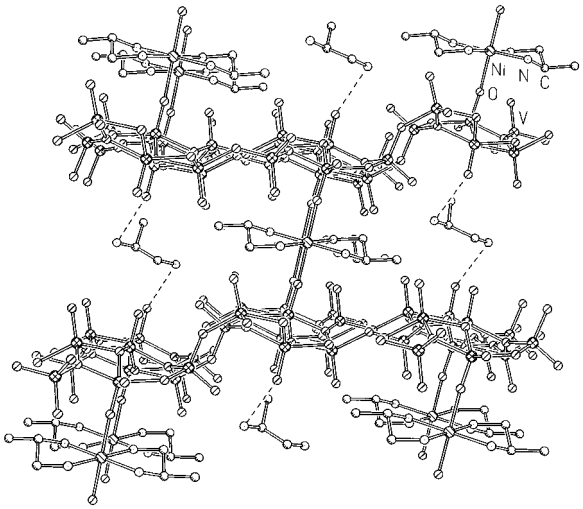

FIGURE 6. View of the structure of $[Ni(enMe)_2]_{0.5}[H_2enMe]_{0.5}[V_6O_{14}]$ down the *a*-axis, showing the layers of vanadium oxide with interlayer $\{Ni(enMe)_2\}^{2+}$ and $\{H_2enMe\}^{2+}$. Reprinted with permission from ref 51. Copyright 1999 American Chemical Society.

interlayer metal coordination complexes, $[Ni(en)_2]_{0.5}[V_3O_7]$ and $[Ni(enMe)_2]_{0.5}[H_2enMe]_{0.5}[V_6O_{14}]$.[51] Both compounds consist of 3D mixed-valence vanadium oxides with interlayers of $\{Ni(en)_2\}^{2+}$, or $\{Ni(enMe)\}^{2+}$ and H_2enMe^{2+}. In the structure of $[Ni(en)_2]_{0.5}[V_3O_7]$, a novel sheet arrangement of vanadium and oxygen atoms of $\{V_3O_7\}^-$ was found with a sheet composition $\{V^{5+}(V^{4+})_2O_7\}^-$. In the structure of $[Ni(enMe)_2]_{0.5}[H_2enMe]_{0.5}[V_6O_{14}]$, both $\{Ni(enMe)\}^{2+}$ and H_2enMe^{2+} serve as unusual pillars between $\{V_6O_{14}\}^{2-}$ sheets. The structure of $[Ni(en)_2]_{0.5}[V_3O_7]$ consists of $\{Ni(en)\}^{2+}$ cations bridged through $\{V_3O_7\}^-$ layers into a 3D framework (Figure 5). The structure of $[Ni(enMe)_2]_{0.5}[H_2enMe]_{0.5}[V_6O_{14}]$ is constructed from $\{Ni(enMe)_2\}^{2+}$ and H_2enMe^{2+} through the $\{V_6O_{14}\}^{2-}$ layer into a 3D framework (Figure 6). It is interesting to see the different arrangements of VO_5 and VO_4 in the inorganic layers. The zigzag chains are arranged in a manner of A−B−A−B through tetrahedral VO_4. In the structure of $[Ni(en)_2]_{0.5}[V_3O_7]$, the direction of the apical oxygen of the neighboring square pyramids is exactly opposite, whereas only the apical oxygens of the middle pyramid are reversed in the case of $[Ni(enMe)_2]_{0.5}[H_2enMe]_{0.5}[V_6O_{14}]$ (Figure 7).

A family of inorganic−organic hybrid compounds with formula $CuL(VO_2)(PO_4)$ (L = 4,4′-bipyridine (4,4′-bipy), 1,10-phenanthroline (1,10-phen), and 2,2′-bipyridine (2,2′-

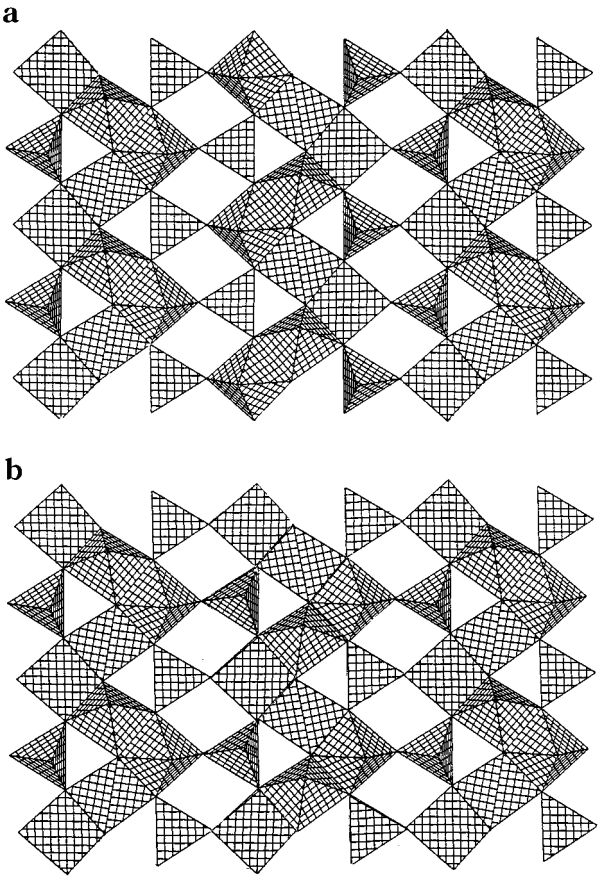

FIGURE 7. View of the vanadium oxide layers of (a) $[Ni(en)_2]_{0.5}[V_3O_7]$ and (b) $[Ni(enMe)_2]_{0.5}[H_2enMe]_{0.5}[V_6O_{14}]$. Reprinted with permission from ref 51. Copyright 1999 American Chemical Society.

bipy)) were hydrothermally synthesized at 160 °C for 120 h.[52] The use of different bidentate organodiamine ligands in the initial reaction systems gave raise to a variety of structures of the products with the same inorganic composition. Cu(4,4′-bipy)$(VO_2)(PO_4)$ and Cu(1,10-phen)-$(VO_2)(PO_4)$ possess the same $\{(VO_2)(PO_4)\}_2$ four-membered rings (4-MRs), whereas the structure of Cu(2,2′-bipy)$(VO_2)(PO_4)$ contains $\{(VO_2)(PO_4)\}_\infty$ infinite chains. The structure of Cu(4,4′-bipy)$(VO_2)(PO_4)$ has a 3D framework, consisting of infinite inorganic layers of $\{CuV_2P_2O_{12}\}_\infty$ (Figure 8a), linked by the coordination of 4,4′-bipy with Cu atoms, as shown in Figure 8b. As expected, the replacement of 4,4′-bipy by 1,10-phen makes the structure change from 3D to 1D. Cu(1,10-phen)$(VO_2)(PO_4)$ is constructed from $\{(VO_2)(PO_4)\}_2^{2-}$ 4-MRs and Cu(1,10-phen)$^{2+}$. A zigzag chain along the *c*-axis is generated in a sequence of $\{CuVPO_3\}$ 3-MRs, $\{V_2P_2O_4\}$ 4-MRs, $\{CuVPO_3\}$ 3-MRs, and $\{Cu_2P_2O_4\}$ 4-MRs (Figure 9). The adjacent chains of $\{Cu(1,10\text{-phen})(VO_2)(PO_4)\}_\infty$ are closely connected through a so-called $\pi-\pi$ interactions of the 1,10-phen. Cu(2,2′-bipy)$(VO_2)(PO_4)$ consists of two $\{(VO_2)(PO_4)\}_\infty$ chains linked by Cu(2,2′-bipy)$^{2+}$ fragments into a pair of 1D chains (Figure 10). These paired chains are aligned in a parallel way and are closely packed.

A hydrothermal reaction of $NaVO_3$, H_3BO_3, $Zn(CH_3COO)_2$, ethylenediamine, and H_2O gives a coordination cluster $[Zn(en)_2]_6[(VO)_{12}O_6B_{18}O_{39}(OH)_3]\cdot 13H_2O$. The structure consists of 18-membered rings of $B_{18}O_{39}(OH)_3$ sandwiched between two alternating edge-sharing vanadium−oxygen clusters V_6O_{15} by six B−(μ_3-O)−V_2 bonds and three B_2-(μ_3-O)−V bonds (see Figure 11). Each of six zinc atoms is coordinated by two ethylenediamine molecules and connected with the $B_{18}O_{39}(OH)_3$ ring by one Zn−(μ_3-O)−B bond. A water molecule occupies the center of the structure. The oxidation states of vanadium in the compound are V(IV) and V(V) in a ratio of 3:1.[53]

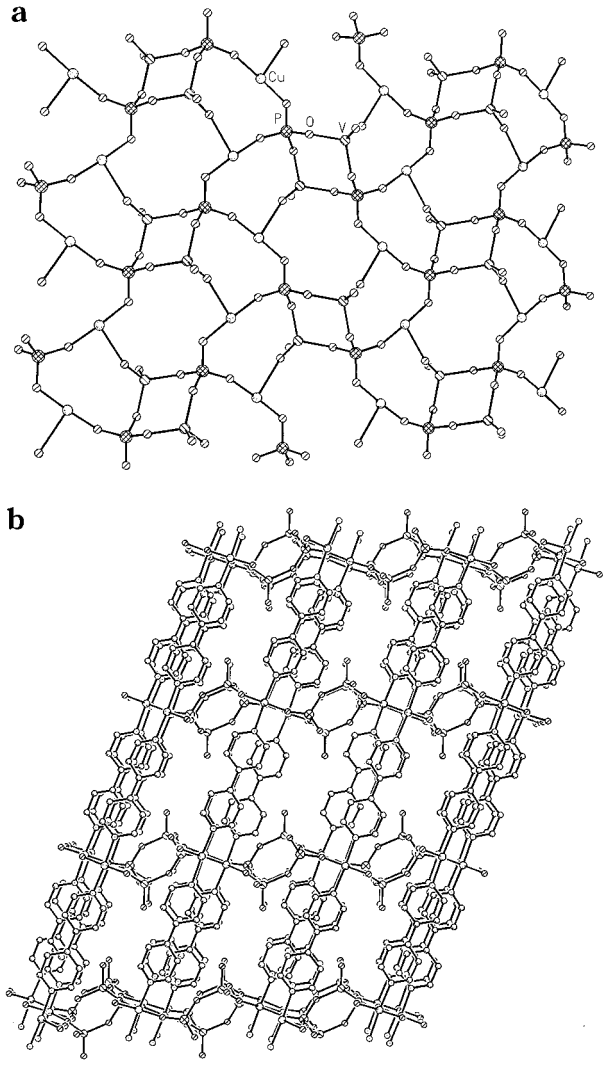

FIGURE 8. (a) View of the $\{CuV_2P_2O_{12}\}$ layer parallel to the *a*-axis. (b) View of the structure of Cu(4,4′-bipy)$(VO_2)(PO_4)$ along the *b*-axis, showing the virtual channels. Reprinted with permission from ref 52. Copyright 2000 American Chemical Society.

Specially Condensed Materials

Hydrothermal synthesis favors the control of morphology, particle size, and elemental valence of synthetic materials by the chemical operations in a specific process of synthesis such as in the synthesis of the nanocrystalline CeO_2-based materials and the mixed-valance GMR material mentioned above. On the other hand, the hydrothermal synthesis is a unique route to specially condensed phases such as superhard materials, helical and chiral structures, and specially arranged coordination states.

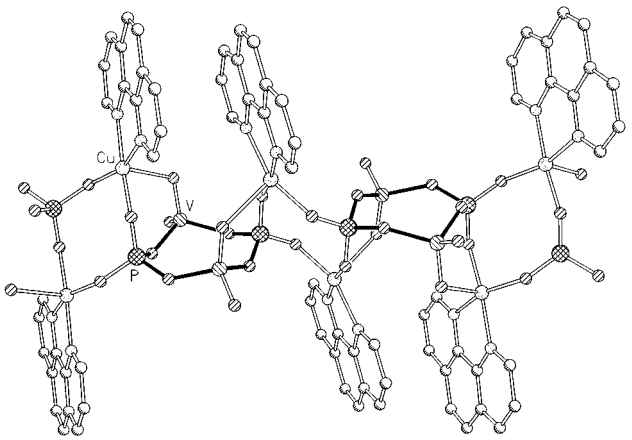

FIGURE 9. View of the 1D chain of Cu(1,10-phen)(VO_2)(PO_4) along the *c*-axis. Reprinted with permission from ref 52. Copyright 2000 American Chemical Society.

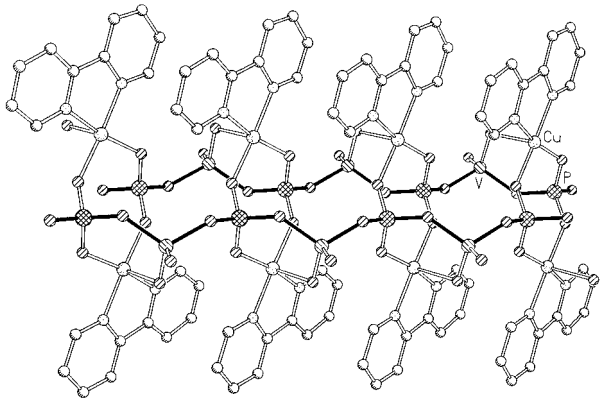

FIGURE 10. Pair of 1D chains of Cu(2,2′-bipy)(VO_2)(PO_4). Reprinted with permission from ref 52. Copyright 2000 American Chemical Society.

Superhard materials such as diamond and gallium nitride (GaN) were recently crystallized from hydrothermal and solvothermal systems, respectively.[54] Apparently, high temperature and high pressure are favorable for diamond as a thermodynamically stable phase. Experimentally, in a typical procedure for diamond growth, powdered nickel, glassy carbon, diamond seeds, and water were sealed in autoclaves and heated at 800 °C and 1.4 kbar. This diamond-on-diamond decomposition under hydrothermal conditions appeared to achieve bigger diamond crystals than the seeds. The solvothermal synthesis of GaN was performed under relatively mild conditions by the reaction of $GaCl_3$ with Li_3N in benzene in an autoclave at 280 °C for 12 h.[55]

Helical or multiple helical structures, which were constructed by a self-assembly of molecules, are often found in nature and are of particular interest in biology and pharmacology. The rational synthesis of inorganic−organic compounds with a helical array is challenging. The most notable has been the hydrothermal synthesis of inorganic double-helix, chiral $[(CH_3)_2NH_2]K_4[V_{10}O_{10}(H_2O)_2(OH)_4(PO_4)_7]\cdot 4H_2O$ reported by Soghomonian et al.[56] This compound was prepared by a hydrothermal treatment of KVO_3, V, H_3PO_4, $CH_3PO(OH)_2$, $(CH_3)_2NH$, and water at 200 °C for 4 days. Its structure consists of a 3D covalently

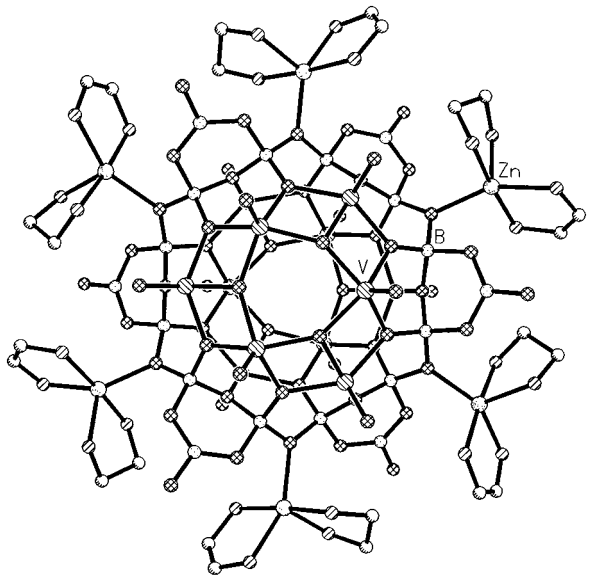

FIGURE 11. View of the structure of $[Zn(en)_2]_6[(VO)_{12}O_6B_{18}O_{39}(OH)_3]\cdot 13H_2O$, showing six $Zn(en)_2$ connected with the $B_{18}V_{12}$ cluster; a water molecule occupies the center of the cluster. Reprinted with permission from ref 53. Copyright 1999 Academic Press.

bonded framework built up from VO_6 octahedra, VO_5 square pyramids, and PO_4 tetrahadra. It contains chiral double helices formed from interpenetrating spirals of V−O pentamers bonded together by P^{5+}. These double helices are in turn intertwined with each other in a manner that generates unusual tunnels and cavities that are filled with $(CH_3)_2NH_2^+$ and K^+ cations, respectively. Three other examples of spirals occur in the hydrothermal product of $RbIn(OH)PO_4$ reported by Lii,[57] a spiral-shaped chain of $[\{Cu(en)(OH_2)\}Mo_5P_2O_{23}]^{4-}$ reported by Lu et al.,[58] and chiral layered *trans*-$Co(dien)_2\cdot Al_3P_4O_{16}\cdot 3H_2O$ (dien = bis-(2-aminoethyl)amine) with a unique six-layer stacking sequence reported by Bruce et al.[59]

A new helix, M(4,4′-bipy)$_2$(VO_2)$_2$(HPO_4)$_4$ (M = Co and Ni; bipy = bipyridine), contains not only an infinite helical chain $[(VO_2)(HPO_4)]_\infty$ but also both left-handed and right-handed helical chains in a structure as shown in Figure 12.[60] This structure was obtained by hydrothermal reaction of $NaVO_3$, NaH_2PO_4, $Co(NO_3)_2$ or $Ni(NO_3)_2$, 4,4′-bipy, and H_2O at 160 °C for 5 days. It has a novel 3D structure constructed from two subunits, e.g., $[(VO_2)(HPO_4)]_\infty$ helical chains and $[M(4,4'\text{-bipy})_2]^{2+}$ fragments. These helical chains are composed of alternating corner-sharing HPO_4 tetrahedra and VO_4N trigonal-bipyramids. The formation of the helix in the structure may be due to the interaction of a rigid [M(4,4′-bipy)$_2$] pillar as an "extra force" with each vanadium atom on the helical chains at a certain angle, ca. 48.5°, which is structurally necessary for stabilizing the helix.

A special five-coordinate titanium was observed in a hydrothermally prepared layered solid, $Na_4Ti_2Si_8O_{22}\cdot 4H_2O$, namely JDF-L1.[61] It is the first synthetic material with five-coordinate titanium, and only one other material, the titanosilicate mineral fresnoite, $Ba_2TiSi_2O_8$, is known to have a structure similar to that of JDF-L1. It was synthesized using tetrabutyl orthotitanate, fumed silica, sodium

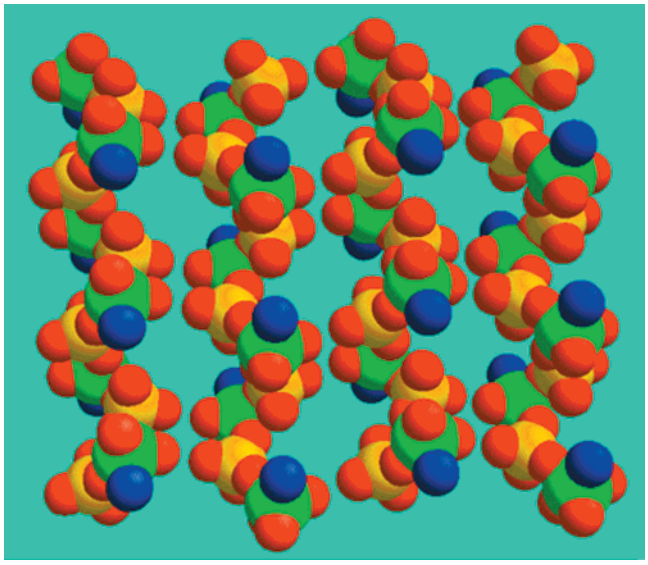

FIGURE 12. View of the space-filling plot of the left-helical and right-helical chains $[(VO_2)(HPO_4)]_\infty$. Color key: V, green; P, yellow; O, red; N, blue. Reprinted with permission from ref 60. Copyright 2000 Wiley.

hydroxide, aqueous hydrogen peroxide, and water as a reaction mixture, which was heated at 180 °C for 10 days. The uniqueness of its structure was found useful in catalyzing hydrocarbon oxidation in the presence of hydrogen peroxide at low temperatures.

Materials, Life, Environment, and Societal Issues

In addition to new materials, currently attractive studies on the origin of life, environmental, and societal issues are increasingly related to hydrothermal synthesis or hydrothermal chemistry. It is hypothesized that rich chemical reactions occurred in the warm sea and all microorganisms have high-temperature ancestors. It is found that most microorganisms living at very high temperatures are archaea on the molecular biological tree. More and more evidence supports the model of the hydrothermal origin of life. However, the most interesting research, such as that into nonenzyme hydrothermal synthesis from inorganic to organic or biological species, needs to be explored further for both deeper understanding of life evolution and possible industrial applications. In contrast to the mild hydrothermal synthesis, the supercritical water oxidation process will effectively decompose almost all organic wastes into smaller molecules and CO_2, serving as a friendly tool for the environment. Accordingly, hydrothermal synthesis (chemistry) provides new materials, helps to clean up our environment, and helps to understand the origin of life.

Conclusions

In summary, a huge number of new materials have been synthesized from hydrothermal systems. The increasing interest in hydrothemal synthesis derives from its advantages in terms of high reactivity of reactants, easy control of solution or interface reactions, formation of metastable and unique condensed phases favored, less air pollution, and low energy consumption. Hydrothermal synthesis has been found to be an effective route for rational synthesis and crystal engineering of microporous crystals, ionic conductors, complex oxides and fluorides, low-dimensional aluminophosphates, inorganic−organic hybrid materials, and particularly condensed materials. These new materials have provoked significant interests in new structural architectures and potential applications to many fields such as photochemistry, electromagnetism, catalysis, and biology.

This work was supported by the National Nature Science Foundation of China (NSFC) and the Ministry of Science and Technology of China (MOSTC).

References

(1) Barrer, R. M. *Hydrothermal Chemistry of Zeolites*; Academic Press: London, 1982.
(2) Demazeau, G. Solvothermal Processes: A Route to the Stabilization of New Materials, *J. Mater. Chem.* **1999**, *9*, 15−18.
(3) Cheetham, A. K.; Ferey, G.; Loiseau, T. Open-Framework Inorganic Materials. *Angew. Chem., Int. Ed. Engl.* **1999**, *38*, 3268−3292.
(4) Li, G.; Li, L.; Feng, S.; Wang, M.; Yao, X. An Effective Synthetic Route for a Novel Electrolyte: Nanocrystalline Solid Solutions of $(CeO_2)_{1-x}(BiO_{1.5})_x$. *Adv. Mater.* **1999**, *11* (*2*), 146−149.
(5) Feng, S.; Greenblatt, M. Galvanic Cell Type Humidity Sensor with Protonic NASICON-Based Material Operative at High Temperature. *Chem. Mater.* **1992**, *4* (*6*), 1257−1262.
(6) Chen, Q. W.; Qian, Y. T.; Chen, Z. Y.; Tang, K. B.; Zhou, G. E.; Zhang, Y. H. Preparation of a Tl-Based Superconductor by a Hydrothermal Method, *Physica C* **1994**, *224* (3−4), 228−230.
(7) Mao, Y.; Li, G.; Xu, W.; Feng, S. Hydrothermal Synthesis and Characterization of Nanocrystalline Pyrochlore Oxides $M_2Sn_2O_7$ (M = La, Bi, Gd or Y). *J. Mater. Chem.* **2000**, *10* (*2*), 479−282.
(8) Zhao, C.; Feng, S.; Chao, Z.; Xu, R.; Shi, C.; Ni, J. Hydrothermal Synthesis of the Complex Fluorides $LiBaF_3$ and $KMgF_3$ with Perovskite Structures under Mild Conditions. *Chem Commun.* **1996**, 1641−1642.
(9) Feng, S.; Wang, D.; Yu, R.; Na, L. Hydrothermal Synthesis Route to a Giant Magnetoresistance Material $La_{0.5}Ba_{0.5}MnO_3$, *Proceedings of the International Symposium on Solvo-Hydro-Thermal Processes*; Org. Comm. Solvothermal Tech. Res.: Takamatsu, Japan, 1997; p12.
(10) Zhao, C.; Feng, S.; Xu, R.; Shi, C.; Ni, J. Hydrothermal Synthesis and Lanthanide Doping of Complex Fluorides $BeBaF_4$, $LiYF_4$ and KYF_4 under Mild Conditions. *Chem. Commun.* **1997**, 945−946.
(11) Baross, J. A.; Deming, J. W. Growth of 'Black Smoker' Bacteria at Temperature of at Least 250 °C. *Nature* **1983**, *303*, 423−426.
(12) Jannasch, H. W.; Mottle, M. J. Geomicrobiology of Deep-Sea Hydrothermal Vents. *Science* **1985**, *229*, 717−725.
(13) Gopalan, S.; Foster, N. R. *Phenol Oxidation in Supercritical Water in MRS*; American Chemical Society: Washengton, DC, 1995.
(14) Wilson, S. T.; Lok, B. M.; Messina, C. A.; Cannan, T. R.; Flanigen, E. M. Aluminophosphate Molecular Sieves: A New Class of Microporous Crystalline Inorganic Solids. *J. Am. Chem. Soc.* **1982**, *104*, 1146−1147.
(15) Parise, J. B. Some Gallium Phosphate Frameworks Related to the Aluminium Phosphate Molecular Sieves: X-Ray Structural Characterization of $\{(PriNH_3)[Ga_4(PO_4)_4OH]\}H_2O^+$. *J. Chem. Soc., Chem. Commun.* **1985**, 606−607.
(16) Yang, G.; Feng, S.; Xu, R. Crystal Structure of the Gallophosphate Framework: X-ray Characterization of $Ga_9P_9O_{36}(OH)\cdot HNEt_3$. *J. Chem. Soc., Chem. Commun.* **1987**, 1254−1255.
(17) Feng, S.; Xu, X.; Yang, G.; Xu, R.; Glasser, F. Hydrothermal Synthesis and Crystal Structure of the Microporous Gallophosphate, $(NH_4)_4[Ga_8P_8O_{32}(OH)_4(H_2O)_4]\cdot 4H_2O\cdot 0.64PrOH$ with an Octahedral−Tetrahedral Framework. *J. Chem. Soc., Dolton Trans.* **1995**, *13*, 2147−2149.
(18) Wang, J.; Feng, S.; Xu, R. The Synthesis and Characterization of a Novel Microporous Alumino-Borate. *J. Chem. Soc., Chem. Commun.* **1989**, 265−266.
(19) Davis, M. E.; Saldarriaga, C.; Montes, C.; Garces, C.; Crowder, C. A Molecular Sieve with 18-Membered Rings. *Nature* **1988**, *331*, 698.

(20) Estermann, M.; McCusker, L. B.; Baerlocher, C.; Merrouche, A.; Kessler, H. A Synthetic Gallophosphate Molecular Sieve with 20-Tetrahydron-Atom Pore Opening. *Nature* **1991**, *352*, 320−322.

(21) Yang, G.; Sevov, S. C. Zinc Phosphate with Gigantic Pores of 24 Tetrahedra. *J. Am. Chem. Soc.* **1999**, *121*, 8389−8390.

(22) Liu, Y.; Du, H.; Xiao, F.; Zhu, G.; Pang, W. Synthesis and Characterization of a Novel Microporous Titanosilicate JLU-1. *Chem. Mater.* **2000**, *12*, 665−670.

(23) Bibby, D. M.; Dale, M. P. Synthesis of Silica-Sodalite from Non-Aqueous Systems. *Nature* **1985**, *317*, 157−158.

(24) Huo, Q.; Feng, S.; Xu, R. First Synthesis of Pentasil-Type Silica Zeolite from Nonaqueous Systems. *J. Chem. Soc., Chem. Commun.* **1988**, 1486−1487.

(25) Huo, Q.; Xu, R.; Li, S.; Ma, Z.; Thomas, J. M.; Jones, R. H.; Chippindale, A. M. Synthesis and Chatacterization of a Novel Extra Large Ring of Aluminophosphate JDF-20. *J. Chem. Soc., Chem. Commun.* **1992**, 875−876.

(26) Yan, W.; Yu, J.; Xu, R.; Zhu, G.; Xiao, F.; Han, Y.; Sugiyama, K.; Terasaki O. $[Al_{12}P_{13}O_{52}]^{3-}[(CH_2)_6N_4H_3]^{3+}$: An Anionic Aluminophosphate Molecular Sieve with Brönsted Acidity. *Chem. Mater.* **2000**, *12*, 2517−2519.

(27) Zhao, H.; Feng, S. Hydrothermal Synthesis and Oxygen Ionic Conductivity of Co-doped Nanocrystalline $Ce_{1-x}M_xBi_{0.4}O_{2.6-x}$, M = Ca, Sr and Ba. *Chem. Mater.* **1999**, *11*, 958−964.

(28) Li, G.; Mao, Y.; Li, L.; Feng, S.; Wang, M.; Yao, X. Solid Solubility and Transport Properties of Nanocrystalline $(CeO_2)_{1-x}(BiO_{1.5})_x$ by Hydrothermal Conditions. *Chem. Mater.* **1999**, *11*, 1259−1266.

(29) Feng, S.; Greenblatt, M. Proton Conductivity and Humidity Sensing Property at High Temperature of a NASICON-Based Material. *Chem. Mater.* **1993**, *5*, 1277−1282.

(30) Pang, G.; Feng, S.; Tang, Y.; Tan, C.; Xu, R. Hydrothermal Synthesis, Characterization, and Ionic Conductivity of Vanadium-Stabilized $Bi_{17}V_3O_{33}$ with Fluorite-Related Superlattice Structure. *Chem. Mater.* **1998**, *10*, 2446−2449.

(31) An, Y.; Feng, S.; Xu, Y.; Xu, R. Hydrothermal Synthesis and Characterization of a New Potassium Phosphatoantimonate, $K_8Sb_8P_2O_{29}\cdot 8H_2O$. *Chem. Mater.* **1996**, *8*, 356−359.

(32) Feng, S.; Tsai, M.; Greenblatt, M. Preparation, Ionic Conductivity and Humidity Sensing Property of Novel Microporous Crystalline Germanates, $Na_3HGe_7O_{16}\cdot xH_2O$, $x = 0-6$, I. *Chem. Mater.* **1992**, *4*, 388−393.

(33) Feng, S.; Greenblatt, M. Preparation, Characterization and Ionic Conductivity of Novel Crystalline Microporous Germanates, $M_3HGe_7O_{16}\cdot xH_2O$, M = Li, NH_4, K, Rb and Cs, II. *Chem. Mater.* **1992**, *4*, 462−468.

(34) Feng, S.; Tsai, M.; Shi, S.; Greenblatt, M. Preparation, Characterization and Ionic Conductivity of Novel Crystalline Microporous Silico-Germanates, $M_3HGe_{7-m}Si_mO_{16}\cdot xH_2O$, M = K, Rb, and Cs, $m = 0-3$, III. *Chem. Mater.* **1992**, *4*, 468−472.

(35) Wu, M.; Long, J.; Wang, G.; Huang, A.; Luo, Y.; Feng, S.; Xu, R. Hydrothermal Synthesis of Tetragnal Barium Titanate from Barium Hydroxide and Titanium Dioxide under Moderate Conditions. *J. Am. Ceram. Soc.* **1999**, *82*, 3254−3256.

(36) Feng, S.; Li, G.; Zhao, C.; Wang, G.; Wang D.; Mao, Y.; Hydrothermal Synthesis of Advanced Complex Oxides and Fluorides, *Proc. 2nd Int. Conf. Solvothermal Reactions*; Org. Comm. Solvothermal Tech. Res.: Takamatsu, Japan, 1996; pp 101−104.

(37) Li, G.; Feng, S.; Li, L.; Li, X.; Jin, W. Mild Hydrothermal Synthesis and Thermal Behaviors of Hydrogarnets, $Sr_3M_2(OH)_{12}$, M = Cr, Fe, and Al. *Chem. Mater.* **1997**, *9*, 2894−2901.

(38) Mao, Y.; Li, G.; Sun, Y.; Feng, S. Hydrothermal Synthesis and Characterization of $Bi_2Pb_2O_7$ with Pyrochlore Structure. *J. Solid State Chem.* **2000**, *149*, 314−319.

(39) Xun, X.; Feng, S.; Wang, J.; Xu, R. Hydrothermal Synthesis of Complex Fluorides $NaHoF_4$ and $NaEuF_4$ with Flourite Structure under Mild Conditions. *Chem. Mater.* **1997**, *9*, 2966−2968.

(40) Xun, X.; Feng, S.; Wang, J.; Xu, R. Hydrothermal Synthesis of Complex Fluorides $LiHoF_4$ and $LiErF_4$ with Scheelite Structures under Mild Conditions. *Mater. Res. Bull.* **1998**, *33*, 369−375.

(41) Sun, J.; Meng, X.; Shi, Y.; Wang, R.; Feng, S.; Jiang, D.; Xu, R.; Xiao, F. A Novel Catalyst of Cu−Bi−V−O Complex in Phenol Hydroxylation with Hydrogen Peroxide. *J. Catal.* **2000**, *193*, 199−206.

(42) Shi, Y.; Feng, S.; Wang, J. Hydrothermal Synthesis of Bi_2MoO_6 and Bi_2WO_6. *Mater. Lett.* **2000**, *44* (3−4), 215−218.

(43) Zhao, H.; Feng, S.; Xu, W.; Shi, Y.; Mao, Y.; Zhu, X. A Rapid Chemical Route to Niobates: Hydrothermal Synthesis and Transport Properties of $Ba_5Nb_4O_{15}$. *J. Mater. Chem.* **2000**, *10* (*4*), 965−968.

(44) Zhou, B.; Yu, J.; Li, J.; Xu, Y.; Xu, W.; Qiu, S.; Xu, R. Rational Design of Two-Dimensional Layered Aluminophosphates with $[Al_3P_4O_{16}]^{3-}$ Stoichiometry. *Chem. Mater.* **1999**, *11*, 1094−1099.

(45) Li, J.; Yu, J.; Yan, W.; Xu, Y.; Xu, W.; Qiu, S.; Xu, R. Structures and Templating Effect in the Formation of 2D Layered Aluminophosphates with $Al_3P_4O_{16}^{3-}$ Stoichiometry. *Chem. Mater.* **1999**, *11*, 2600−2606.

(46) Yu, J.; Xu, R.; Li, J. Structural Diversity of a Family of Aluminophosphates with Al/P Ratio of Non-Unity. *Solid State Sci.* **2000**, *2*, 181−192.

(47) Janiak, C. Functional Organic Analogues of Zeolites Based on Metal−Organic Coordination Frameworks. *Angew. Chem., Int. Ed. Engl.* **1997**, *36*, 1431−1434.

(48) Batten, S. R.; Robson, R. Interpenetrating Nets: Ordered, Periodic Entanglement. *Angew. Chem., Int. Ed.* **1998**, *37*, 1460−1494.

(49) Yaghi, O. M.; Li, H.; Davis, C.; Richardson, D.; Groy, T. L. Synthetic Strategies, Structure Patterns, and Emerging Properties in the Chemistry of Modular Porous Solids. *Acc. Chem. Res.* **1998**, *31*, 474−484.

(50) Hagrman, P. J.; Hagrman, D.; Zubieta, J. Organic−Inorganic Hybrid Materials: From "Simple" Coordination Polymers to Organodiamine-Templated Molybdenum Oxides. *Angew. Chem., Int. Ed.* **1999**, *38*, 2638−2684.

(51) Shi, Z.; Zhang, L.; Zhu, G.; Yang, G.; Hua, J.; Ding, H.; Feng, S. Inorganic/Organic Hybrid Materials: Layered Vanadium Oxides with Interlayer Metal Coordination Complexes. *Chem. Mater.* **1999**, *11*, 3565−3570.

(52) Shi, Z.; Feng, S.; Zhang, L.; Yang, G.; Hua, J. Hydrothermal Syntheses and X-ray Crystal Structures of Three Inorganic−Organic Hybrid Materials in a Copper Vanadium Phosphate Family: $CuL(VO_2)(PO_4)$ (L = 4,4′-bipy, 1,10-phen, 2,2′-bipy). *Chem. Mater.* **2000**, *12*, 2930−2935.

(53) Zhang, L.; Shi, Z.; Yang, G.; Chen, X.; Feng, S. Hydrothermal Synthesis and X-ray Crystal Structure of $[Zn(en)_2][(VO)_{12}O_6B_{18}O_{39}(OH)_3]\cdot 13H_2O$. *J. Solid State Chem.* **1999**, *148*, 450−454.

(54) Zhao, X.; Roy, R.; Cherian, K. A.; Badzian, A. Hydrothermal Growth of Diamond in Metal−C−H_2O Systems. *Nature* **1997**, *385*, 513−515.

(55) Xie, Y.; Qian, Y.; Wang, W.; Zhang, S.; Zhang, Y. A Benzene-Thermal Synthetic Route to Nanocrystalline GaN. *Science* **1996**, *272*, 1926−1927.

(56) Soghomonian, V.; Chen, Q,; Haushalter, R. C.; Zubieta, J.; O'Connor, C. J. An Inorganic Double Helix: Hydrothermal Synthesis, Structure, and Magnetism of Chiral $[(CH_3)_2NH_2]K_4[V_{10}O_{10}(H_2O)_2(OH)_4(PO_4)_7]\cdot 4H_2O$. *Science* **1993**, *259*, 1596−1599.

(57) Lii, K. H. $RbIn(OH)PO_4$: An Indium(III) Phosphate Containing Spirals of Corner-Sharing InO_6 Octahedra. *J. Chem. Soc., Dalton. Trans.* **1996**, 815−818.

(58) Lu, J.; Xu, Y.; Goh, N. K.; Chia, L. S. Hydrothermal Assembly and Structural Characterisation of One- and Two-Dimensional Organic/Inorganic Hybrid Materials Constructed from Diphosphopentamolydbate(VI) Clusters and $[Cu(en)]^{2+}$ Complex Groups. *Chem. Commun.* **1998**, 2733−2734.

(59) Bruce, D. A.; Wilkinson, A. P.; White, M. G.; Bertrand, J. A. The Synthesis and Characterization of an Aluminophosphate with Chiral Layers: Trans-$Co(dien)_2\cdot Al_3P_4O_{16}\cdot 3H_2O$. *J. Solid State Chem.* **1996**, *125*, 228−233.

(60) Shi, Z.; Feng, S.; Zhang, L.; Gao, S.; Yang, G.; Hua, J. Inorganic−Organic Hybrid Materials Constructed from $[(VO_2)(HPO_4)]_\infty$ Helical Chains and $[M(4,4'\text{-bipy})_2]^{2+}$ (M = Co, Ni) Fragments, *Angew. Chem., Int. Ed.* **2000**, *39* (13), 2325−2327.

(61) Roberts, M. A.; Sankar, G.; Thomas, J. M.; Jones, R. H.; Du, H.; Chen, J.; Pang, W.; Xu, R. Sythesis and Structure of a Layered Titanosilicate Catalyst with Five-Coordinate Titanium. *Nature* **1996**, *381*, 401−404.

AR0000105